Reprinted from

JOURNAL OF HYDROLOGY

Journal of Hydrology 194 (1997) 15–37

Linking space–time scale in hydrological modelling with respect to global climate change
Part 1. Models, model properties, and experimental design

Dionysia Panagoulia[a,*], George Dimou[b]

[a]*National Technical University of Athens, Department of Civil Engineering, Division of Water Resources–Hydraulic and Maritime Engineering, 5 Iroon Polytechniou, 15780 Zographou, Athens, Greece*
[b]*7 Voutyra, 16673 Voula, Athens, Greece*

Received 10 July 1995; revised 20 June 1996; accepted 24 June 1996

ELSEVIER

is a complicated problem owing to the immense range of scales involved, and the differences that appear when the phenomena are viewed at different space and time scales (Global Atmospheric Research Programme, 1972; Smagorinsky, 1974; Dooge, 1982, 1986, 1992). A complete theory of hydrology, relevant to climate modelling, would have to cover phenomena from the scale of the water molecule to the grid scale of the general circulation model (GCM).

Thus, to build up a model at a given scale, one must either (1) parameterize laws established at a lower microscale to predict the key variables at the required scale, and (2) disaggregate models validated at a higher scale to produce more detailed predictions at the required scale, or (3) attempt to establish new laws at the required scale and validate them by measurements at this scale. Parameterizing from the scale of hydrological physics to the GCM scale involves several levels of parameterization (Dooge, 1982, 1992), and this task remains an active but difficult area for hydrological research. The upscaling of land-surface hydrological processes is related to the large-scale field experiments, such as the ECHIVAL (European International Project on Climate and Hydrological Interactions between Vegetation, Atmosphere, and Land Surfaces), the EFEDA (ECHIVAL Field Experiment in Desertification-Threatened Area) and the HAPEX (Hydrologic–Atmosphere Pilot Experiment) (BAHC Core Project Office, 1993), that are carried out today to test the GCM predictions under the forcing of global climate change.

Another important feature is the connection of scales in space and time. The link between time and space scales is intrinsic because the meteorological–hydrological processes (e.g. rainfall–runoff) are highly non-linear in both space and time, particularly in catchment storm response modelling (Lettenmaier et al., 1988; Panagoulia, 1991, 1992a). Furthermore, other processes, such as infiltration and evapotranspiration, which play major roles in the runoff of a catchment, depend strongly on the storage and movement of water within the soil column during storms, as well as the soil moisture condition at the onset of storms. The latter implies a strong compatibility between space and time scales (Becker and Nemec, 1987; Lettenmaier et al., 1988; Becker, 1992; Sunada, 1993).

The above-mentioned qualitative aspects of scales become more pressing when hydrological processes in a mountainous area have to be modelled. In mountainous regions the progress of various hydrological phenomena is faster than in lowlands, mainly because of greater hydraulic gradients, greater flow velocities and faster transmission of hydraulic impulses. This results in a higher range of streamflow fluctuation, requiring for catchment representation more physical and finer-grid models than are required for flat areas of comparable size (Klemes, 1990; Silar, 1990).

Although an appropriate link between space and time scale should be maintained, it is often disregarded in hydrological research and the scales are chosen independently. Consequently, modelling of physical processes becomes less realistic, and predictions are more difficult to understand. This case is shown here and in the companion paper, where the effects of global climate change at the scale of medium-sized catchments in a mountainous environment are to be interpreted.

Two modelling approaches with different time resolution were used for the same catchment. The first approach, used by Mimikou and Kouvopoulos (1991) and Mimikou et al. (1991), is a monthly water balance (MWB) model which includes a snowmelt

component. The second approach is based on the coupling of the US National Weather Service (US NWS) snow accumulation–ablation (SAA) model and the soil moisture accounting (SMA) model of Panagoulia (1991, 1992a,b, 1993) and Panagoulia and Dimou (1994b). The SAA model ran on a 6 h step, whereas the SMA model was operated on a daily step.

Concerning the laws governing each approach, the models are rather differently structured. This is an additional reason to believe in the different behaviour of the two approaches with respect to global climate change. Under these circumstances, the comparison of the models is an important part of the paper's objectives.

In the present paper, the relative contributions of snowmelt and flow to streamflow for the MWB and SAA–SMA models were examined and compared. In addition, the parameter calibration and estimation issues for both the MWB and SAA–SMA models are discussed, as well as the models' reliability with respect to measured flows. The results from the monthly streamflow and soil moisture simulations generated from both approaches with historical input data are presented.

In the companion paper (Panagoulia and Dimou, 1997), a comparative analysis of hydrological results (streamflow and soil moisture) for the MWB and SAA–SMA models is performed. The input was adjusted for a set of hypothetical climate change scenarios. The differences between the MWB and SAA–SMA results are presented in detail.

In an early estimation of climate change effects, Gleick (1986, 1987) developed a two-zone (high elevation and low elevation) water balance model. This two-zone approach operated on a monthly time step, which was fully compatible with the basin scale (40 000 km^2) where the model was applied. Mimikou and Kouvopoulos (1991) and Mimikou et al. (1991) implemented a monthly water balance model for climate change studies, but the time resolution of the model was incompatible with the catchment scale under simulation (633 km^2). The consequences of this inconsistency have been analysed here and in the companion paper. The SAA–SMA models have been successfully applied for climate change interpretation. Lettenmaier et al. (1988), Lettenmaier and Gan (1990), Panagoulia (1991, 1992a, 1993) and Panagoulia and Dimou (1994a,b) have implemented them on the appropriate catchment scale, and Bae and Georgakakos (1994), as well as Georgakakos and Bae (1994), have made some modifications in several formulations of the SMA model to apply it over three large drainage basins (ranging from 2000 to 3500 km^2) of the Midwestern USA.

The models are examined and compared in the next section. The study catchment is described and the available data are given in Section 3. In Section 4, the parameter estimation is presented, and the model calibration and validation with historical data for both approaches is discussed. The numerical index (NTD) and the monthly values of compared streamflow are given in Section 5. Conclusions are presented in Section 6.

2. Hydrological models

Two parts were clearly identified in the models which were examined. The first part, which represented the snow accumulation and ablation, constitutes a component for the MWB model and a whole model for the US NWS, i.e. the SAA model. The second part,

which represented the soil-level water balance over the catchment, is the main body of the MWB model and also a whole model for the US NWS, i.e. the SMA model. The yielded quantity 'rain plus melt' from both models was used as input to the MWB soil-level component and the SMA model, respectively. In the second part of the examined models the balance was expressed among the moisture content of the soil divided into one or more zones (upper, lower, etc.), and the incoming (rain plus melt) and outgoing (evapotranspiration and runoff) quantities.

The differences between the MWB and SAA–SMA models which are described in the present study relate to snow accumulation and melt, the runoff production through the various mechanisms of water balance at soil level, and percolation and actual evapotranspiration. A brief description of models' operation is given in the following sections.

2.1. Monthly water balance (MWB) model

Water balance models were initially developed in the 1940s and 1950s by Thornthwaite and Mather (1955, 1957). Since then, water balance models have been adopted and applied to a variety of hydrological regimes (Thornthwaite and Mather, 1955; Mather, 1978; Hayes et al., 1980). They can incorporate soil moisture, evapotranspiration and snowfall–snowmelt parameters, giving the sense of conceptually operated models. In reality, they are quasi-conceptual models and are not included in the well-known conceptual models (Clarke, 1973; Fleming, 1975; WMO, 1975; Manley, 1978; Franchini and Pacciani, 1991). They are also general models and they have to be calibrated for a particular catchment. The examined water balance model requires the monthly average air temperature, precipitation and potential evapotranspiration as inputs, as well as the measured monthly streamflow against which the model estimated streamflow is compared. The MWB model parameters are adjusted until the model output streamflow resembles, according to some evaluative criterion (mean square error, Nash parameter NTD, etc.), the measured catchment total runoff (streamflow). The main output of the model is the estimated streamflow and the soil moisture.

The components of the MWB model are presented in Fig. 1. At a monthly time step, the model estimates the potential evapotranspiration (PET) from the Blaney–Criddle equation (FAO, 1977), divides precipitation (P) by rain (RA) and snow (SN) according to the monthly average air temperature (T_a), and calculates storm runoff (Q_s) before evapotranspiration or infiltration takes place. The remaining quantity of rain water ($RA - Q_s$) plus the quantity of snowmelt (SNM), if any, first satisfies the demand for evapotranspiration (ET) and then saturates the soil moisture. If the quantity ($RA + \mathrm{SNM} - Q_s$) is not adequate to satisfy the PET, then an amount of water is drawn from the soil moisture of the previous month. In the opposite case, after the soil moisture is saturated ($S = S_{max}$), the surplus water (SW) is subdivided into overland flow (or interflow) and groundwater (G). G contributes to streamflow through the baseflow (K_2G) with a lag of 1 month. Thus, the total estimated monthly runoff ($QE(t)$) at the month t is the sum of storm runoff $Q_s(t)$, the surplus water $K_1SW(t)$ and baseflow $K_2G(t-1)$: $QE(t) = Q_s(t) + K_1SW(t) + K_2G(t-1)$. The eight parameters involved in the MWB model are described in the section on model calibration.

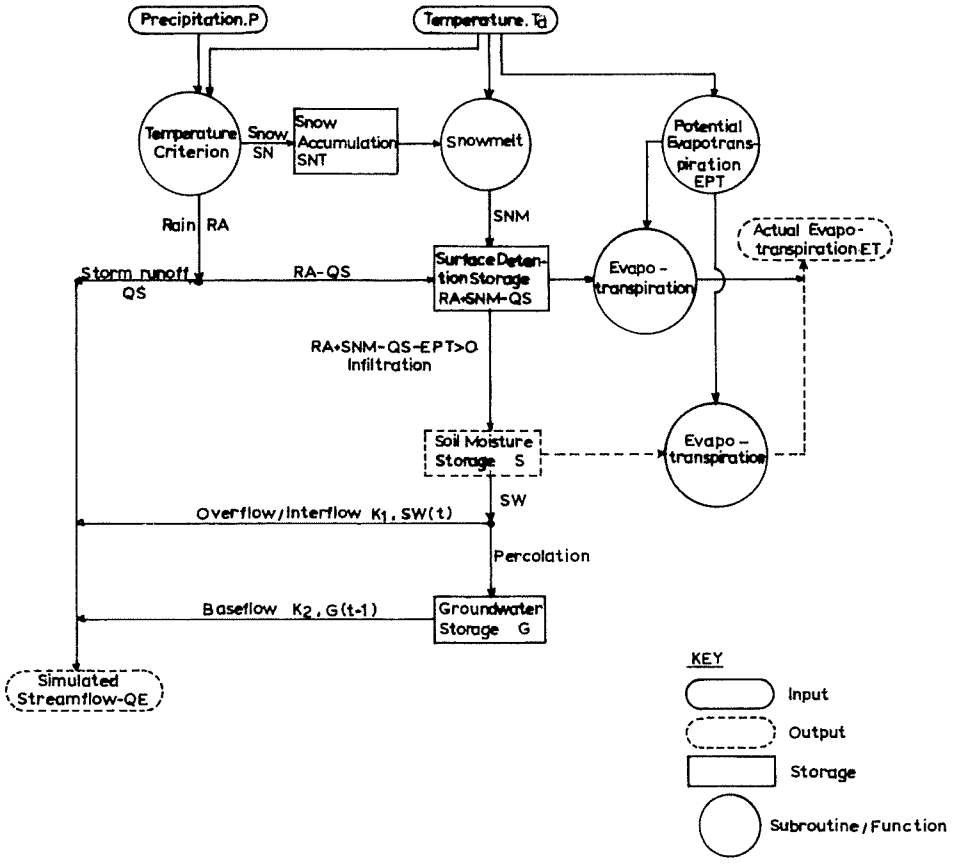

Fig. 1. Monthly water balance model components.

2.2. *Snow accumulation and ablation (SAA) model*

The SAA model was developed by Eric Anderson, of the US National Weather Service Hydrologic Research Laboratory (Anderson, 1973), and has been tested in numerous mountainous watersheds in the USA and elsewhere. It is a deterministic, continuous conceptual model consisting of a set of mathematical formulations which describe explicitly the accumulation and ablation of the snowpack. The model itself can be coupled with almost any soil moisture accounting (rainfall–runoff) model. The output 'rain plus melt' from the SAA model can be the input to the rainfall–runoff model. The model inputs are air temperature and precipitation at a 6 h time step. For the SAA analysed model, daily precipitation was interpolated to 6 h increments and 6 h temperature was estimated from daily temperature maxima and minima using equations given by Anderson (1973). The calibration of the SAA model was performed concurrently with any rainfall–runoff model, as the SAA model provides the input to the rainfall–runoff model, which in the case examined is the US NWS soil moisture accounting model.

The structure of the SAA model presented in Fig. 2 can be summarized as follows.

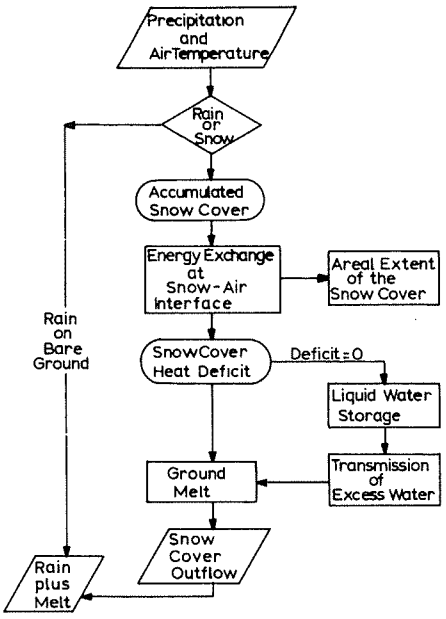

Fig. 2. Snow accumulation and ablation model components.

When air temperature (T_a) is less than the delineation temperature (0°C or other), accumulation of snowpack occurs. In the opposite case (T_a greater than delineation temperature), the SAA model assumes that the precipitation is rain. The ablation of snowpack is controlled by the heat exchange at the air–snow interface. For the heat exchange computations there are two basic conditions: (1) when $T_a > 0$°C, melt takes place at the snow surface; (2) when $T_a < 0$°C, melt occurs. Yet the melt is computed for rain or non-rain periods. For melt during rain periods the following assumptions are made: (1) there is no solar radiation; (2) incoming longwave radiation is equivalent to blackbody longwave radiation at T_a; (3) snow surface temperature is 0°C; (4) the dew point is T_a; (5) the rain temperature is T_a. Under these assumptions, the amount of melting snowpack expressed as heat losses (ΔQ) is the sum of longwave radiation (Q_n), latent heat transfer owing to condensation (Q_e), sensible heat transfer (Q_h) and heat transfer by rain water (Q_{px}): ($\Delta Q = Q_n + Q_e + Q_h + Q_{px}$.

For melt during non-rain periods, the model checks whether the snowpack is isothermal at 0°C. If the snowpack is not isothermal, no melt occurs. If the snowpack is isothermal and $T_a > 0$°C, melt occurs at a rate proportional to a seasonally varying melt factor and the difference between T_a and 0°C.

During non-melt periods, an antecedent temperature index (ATI) is used as an index to the temperature of the surface layer of the snowpack. The heat exchange is assumed proportional to the temperature gradient, which varies seasonally, as does the melt factor of non-rain periods.

The SAA model accounts also for the areal extent of snow cover. During the periods of snow accumulation, this is assumed to be 100%. During periods of depletion, the model

uses an areal depletion curve of snow. The SAA model involves six major and six minor parameters that are described in the section on model calibration.

2.3. Soil moisture accounting (SMA) model

The soil moisture accounting (SMA) model was developed by Burnash et al. (1973) and forms the basis of the US National Weather Service's basic catchment hydrological response model for operational forecasting. At first, the SMA model was used for the Sacramento River basin simulation, and since then it has been widely used (e.g. WMO, 1975; Nemec and Kite, 1981; Gupta and Sorooshian, 1983; Lettenmaier et al., 1988; Panagoulia, 1991, 1992a,b). The SMA model can be classified using Clarke's scheme (Clarke, 1973) as a deterministic, explicit, continuous, lumped-parameter, conceptual model. However, the dynamically expanding saturated surface area (ADIMP) as one of the SMA model's important parameters and associated with the additional direct runoff genesis gives spatially distributed characteristics to the model.

The original SMA model was designed for daily precipitation input, but later versions allow finer time increments (6 h or less). The input to the SMA model is the daily pseudo-precipitation (rain plus SAA model output) and the potential evapotranspiration (actual or long-term average). The latter, in the examined model, was estimated through the Penman method (Veihmeyer, 1964). The SMA model is based on a system of percolation, soil moisture storage, drainage and evapotranspiration characteristics, to represent the significant hydrological process in a rational manner. The definition of the model parameters is achieved by establishing a soil-moisture computation which allows the determination of watershed streamflow from watershed precipitation. Effective moisture storage capacities in the soil profile are estimated not by sampling of the soil profile, but by inference from the pseudo-precipitation and streamflow records. The final values of the model parameters are determined through the calibration procedure.

Fig. 3 illustrates the components of the SMA model. The model is represented by an upper and lower zone. Each zone stores moisture in two forms, tension moisture and free moisture. Tension moisture denotes water closely bound to the soil particles whereas free moisture is the moisture that fills the soil pores. The upper zone includes one free moisture storage whereas the lower zone includes two free moisture storages (primary and supplemental).

Free water from the upper zone can descend to the lower storages by percolation or can move laterally to produce interflow. Percolation is controlled by the contents of the upper zone free water and the deficiency of lower zone moisture volume. When the precipitation rate exceeds the percolation rate and the maximum interflow drainage capacity, then the upper zone free water capacity is filled completely and the excess rainfall will result in surface runoff.

The two lower free water storages fill simultaneously from percolated water, and drain independently at a different rate, giving a variable groundwater recession. Moisture is also extracted from the upper and lower tension zones and from free water surfaces by evapotranspiration. Direct runoff from impervious areas, surface runoff, interflow, and primary and supplemental baseflow contribute to generate the channel flow. The SMA model includes about 21 parameters, which are discussed in the section on model calibration.

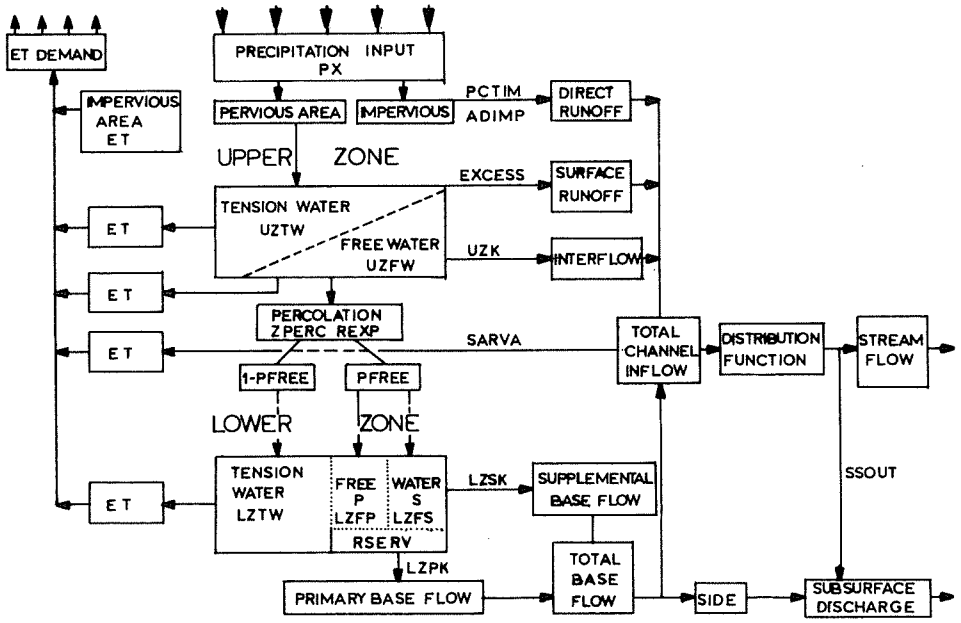

Fig. 3. Soil moisture accounting model components.

2.4. *Differences in the structure of the SAA and MWB-snow models*

As seen from Fig. 2, several physical components are represented in the SAA model. The calculation of snowmelt is the most important part of the SAA model, because the snowmelt process controls the rate at which water is released from the snowpack to the land phase of the hydrological cycle, which has a dominant effect on the resulting hydrograph. The accumulation of the snowpack is also important, especially in terms of water equivalent, because it influences the total runoff volume. Equally important is the areal extent of the snow cover, as it controls the area contributing to the runoff process. Whereas the remaining SAA model components are less important, they are restrictive in many watersheds. The MWB-snow model accounts for only a rough representation of snow accumulation and melt components. The differences in snow accumulation and melt components in the SAA and MWB models are described below.

2.4.1. *Accumulation of the snowpack*

The SAA model uses the ambient 6 h air temperature ($T_{a,6\,h}$) to estimate the form of precipitation. A model parameter (PXTEMP, °C) indicates the temperature which delineates rain from snow. When $T_{a,6\,h} >$ PXTEMP, the precipitation is rain, and when $T_{a,6h} \leq$ PXTEMP the precipitation is snow. Because the measurements of precipitation gauges are biased during snowfall periods the model uses a mean snowfall correction factor (SCF). Thus, precipitation which is classified as snow is adjusted with the SCF (model parameter) and added to the existing snowpack. Rain which falls on bare ground immediately enters the SMA model. Rain falling on the snowpack is added to the computed surface melt water.

In the MWB-snow model two temperature limits (model parameters) are included, T_0 (°C) and T_1. When the monthly air temperature ($T_{a,m}$) is below T_0 the snow content reaches its maximum value. When $T_0 < T_{a,m} < T_1$ the snow content is linearly dependent on $T_{a,m}$ and when $T_{a,m} > T_1$ the precipitation (P) falls entirely as rain. The model also assumes a minimum rain content (RA) when $T_{a,m} \leq T_0$. In this case, precipitation is adjusted by the minimum rain content coefficient (α): $RA = \alpha P$. The MWB model does not account for rain falling on bare or snow-covered ground as does the SAA model. In the MWB model the precipitation amount falling as rain is adjusted by the monthly coefficient of direct runoff (SRC) to produce storm runoff.

2.4.2. Snowmelt

In the MWB model, the quantity of snow melting (SNM) is computed through the degree-day method, each month, which uses air temperature as an index to snowpack (snowtank (SNT) in the MWB model) outflow. This is very different from the SAA model, which uses the air temperature as an index to energy exchange across the snow–air interface.

The degree-day method does not explicitly account for those processes (the freezing of melt water owing to a heat deficit, and the retention and transmission of liquid water, processes parameterized in the SAA model) which cause snowpack outflow to differ from snowmelt. Furthermore, the MWB-snow model does not distinguish the melting during rain or non-rain periods, as well as the heat exchange during melt or non-melt periods, processes separated and explicitly described in the SAA model. A complete description of the SAA model algorithms has been given by Anderson (1973).

2.5. Differences in the structure of the SMA and MWB-runoff models

As seen from Fig. 3, the SMA model considers the entire catchment hydrology, from precipitation to stream discharge, as a series of interlinked processes and moisture storages in various soil levels. The processes of the catchment are described mathematically and the storages are considered as reservoirs in which water balance is maintained. In the MWB-runoff model (Fig. 1), the interlinked processes are poorly or not at all represented, and the number of moisture storages is very limited without any clear separation into soil levels. The differences in the streamflow components (produced by the balance of moisture storages at soil level) and in the interlinked processes (actual evapotranspiration and percolation) in the SMA and MWB-runoff models are described in the following section.

2.5.1. Soil-level water balance

In the SMA model the direct surface runoff is expressed as a percentage of catchment surface, which varies from a minimum value (percentage of impervious surface depends only on the nature of the land) to a maximum value (percentage of marshes and temporary areas of stagnation). In the MWB-runoff model the direct surface runoff is expressed through a storm runoff coefficient depending on the morphology and the soil characteristics of the catchment. The coefficient varies from month to month in the year.

The SMA model reproduces the surface runoff by evaluating the excess storage capacity attributed to the free water reservoir of the upper soil zone. This storage capacity is

considered constant over the entire catchment. The MWB-runoff model uses one level (layer) in which soil moisture is treated as a storage layer with corresponding inflows and outflows. Inflow results from infiltration into the soil, pseudo-precipitation (rain plus melt) minus storm runoff, and upward flow owing to plant action or saturation flow. Outflow results from *ET* and percolation to subsurface flows or groundwater. Under this parameterization of the MWB-runoff components, the surface runoff is described as an overflow or interflow, terms which are not distinguished.

In the SMA model the interflow is proportional to the free water volume remaining after percolation, i.e. interflow = UZK × UZFWC, where UZK is the upper zone free water storage depletion coefficient, and UZFWC is the volume of free water stored in the upper zone. In the MWB-runoff model the interflow associated with overflow is evaluated as a percentage of surplus water, which is the quantity of water remaining after storm runoff, evapotranspiration and replenishing soil moisture. This percentage expresses the catchment lag or catchment detention factor, estimated depending on the catchment size.

The lower zone in the SMA model (Fig. 3) represents a groundwater reservoir including two free water reservoirs (primary and supplemental). The primary reservoir contributes to the actual baseflow component, and the supplemental to the component intermediate between the interflow and the baseflow. These reservoirs are assumed to be linear and the combined baseflow is equal to: [(Volume 1) (Drainage Factor 1)] + [(Volume 2) (Drainage Factor 2)] where Volume 1 is identified as the primary reservoir and Volume 2 as the supplemental reservoir. In the MWB-runoff model the groundwater storage behaves like a reservoir receiving a percentage of the surplus water and contributing to the channel inflow by baseflow with a time lag of 1 month.

2.5.2. Evapotranspiration

In the SMA model, evapotranspiration (*ET*) takes place from the upper and lower zone, as well as from the portion of the catchment area which acts as an impervious surface when it is saturated (Fig. 3). *ET* from the upper zone first takes place at the level of the tension water reservoir at a rate proportional to the moisture content and the capacity of the reservoir. Whenever the *ET* requirement is not completely satisfied, moisture is withdrawn from the free water reservoir at the potential rate. Any further demand for *ET* is addressed to the lower zone tension water reservoir. The actual *ET* from this reservoir takes place at a rate proportional to the contents of the reservoir and the sum of the capacities of both upper and lower tension water reservoirs. *ET* from the area which acts as an impervious surface is assumed to be equal to that from the upper zone tension water reservoir plus a moisture quantity which is proportional to the moisture contents and the sum of the tension water capacities.

There are two stages of *ET* in the MWB-runoff model. When the soil moisture is greater than the field capacity (S_{max}), *ET* proceeds at the potential rate and depends on meteorological factors. When the soil moisture content has decreased below the maximum value (S_{max}), the rate of *ET* is a linear function of the moisture content of the soil. When the difference between pseudo-precipitation (rain plus melt) and storm runoff exceeds the potential *ET*, the rate of the actual *ET* is equal to the potential rate, and the available surplus water for runoff is a function of the soil moisture. When soil moisture is below S_{max}, the surplus water is equal to the pseudo-precipitation minus the storm runoff minus

the *ET* minus the change in soil moisture. In the opposite case, when the difference between pseudo-precipitation and storm runoff is less than the potential *ET*, the actual *ET* is equal to the above difference plus the change in soil moisture, and there is no surplus runoff.

2.5.3. Percolation process

Percolation in the SMA model, where the soil water moves from the upper zone to the lower zone, is evaluated by the following equations:

$$\text{Percolation} = \text{Perc}[1 + \text{ZPERC}(\text{Deficiency})^{\text{Rexp}}]$$

$$\text{Perc} = \frac{(\text{LZFPM} \times \text{LZPK} + \text{LZFSM} \times \text{LZSK})\ \text{UZFWC}}{\text{UZFWM}}$$

where LZFPM is the lower zone free maximum primary storage, which is the maximum storage capacity for slower drainage baseflow, LZPK is the lower zone primary storage depletion coefficient, LZFSM is the lower zone free water maximum supplemental storage, which is the maximum capacity for faster draining baseflow, and LZSK is the lower zone supplemental storage depletion coefficient. ZPERC is a factor used to increase the percolation potential from the minimum (Perc) to the maximum Perc(1 + ZPERC). UZFWC and UZFWM are the volume of the upper zone free water at the present content and the maximum level correspondingly.

The above equations are not included in the MWB-runoff model, which, in addition, does not include any infiltration or groundwater equation for moving water from the surface detention storage to the soil moisture storage and consequently to groundwater storage (Fig. 1).

2.5.4. Transfer to the closure section of the catchment

In the SMA model the direct runoff, surface runoff, interflow, and baseflow are produced separately. The sum of these runoff components is transferred to the closure section of the catchment by using a dimensionless unit hydrograph. This transfer process is not included in the MWB-runoff model, which adds the overflow or interflow and baseflow directly to the storm runoff to form the total runoff in the closure section of the catchment.

2.5.5. Summary

The structural differences of the snow accumulation and ablation components, the soil-level water balance components and the interlinked processes have been outlined to explain in part why there may be differences in streamflows (hydrographs) simulated with the MWB and the SMA model, although both models were operated on the same time step and calibrated with error-free climatic inputs.

3. Catchment features and input data

The Mesochora catchment, which is drained by the upper Acheloos river, was used for analysis and comparison of the MWB and the SAA–SMA model. The Mesochora is of

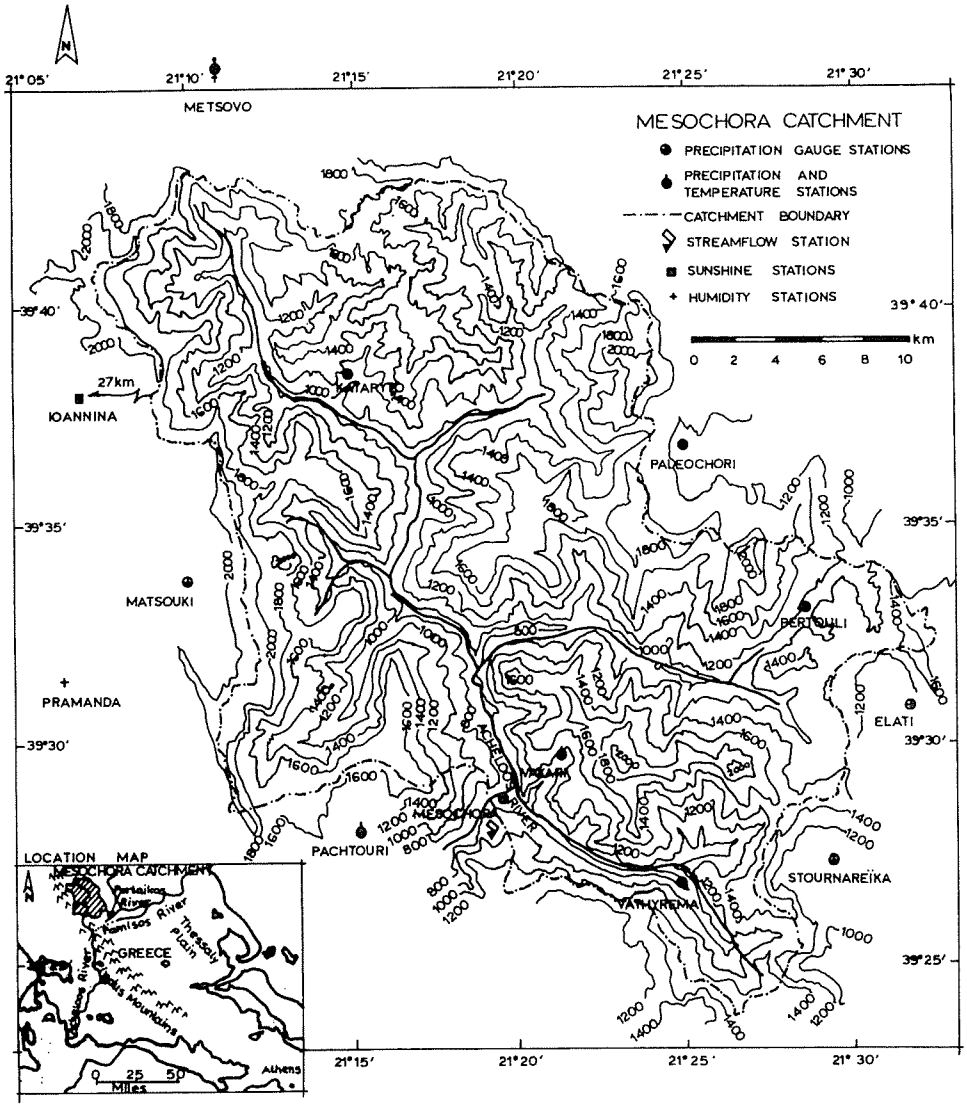

Fig. 4. The Mesochora catchment in Greece and recording stations.

great significance for Greece because the river will be partially diverted at the outfall of the catchment through the Pindus mountains to irrigate the arid Thessaly Plain. This is the largest project in Greece, and includes five dams (one is the Mesochora dam), 24 miles of large tunnels and about 5000 miles of buried irrigation pipes.

The Mesochora catchment lies in the central mountain region of Greece and extends from north (39°42′) to south (39°25′), with an area of about 633 km^2 (Fig. 4) belonging to catchment space scale of 100–1000 km^2 (Becker and Nemec, 1987; Lettenmaier and Gan, 1990). The mean elevation is 1390 m and the climate is elevation dependent, with hot

summers and mild winters at low elevations, and mild summers and cold winters at high elevations. The catchment hydrology is controlled by snowfall and snowmelt at high elevations.

The network of meteorological stations (precipitation, temperature, sunshine, humidity and wind) installed in and around the catchment is relatively dense. However, some daily values, particularly of precipitation and minimum and maximum temperature time series for the 15 year study period (1972–1986), have not been recorded. The mean annual precipitation (rain plus melt) weighted over elevation bands is 1900 mm, and the catchment's runoff is 1170 mm. A more detailed description of the catchment has been presented by Panagoulia (1992b). The measured data and the methods used to average the data over the area and the elevation are presented in the following sections for both the MWB and SAA–SMA models.

3.1. MWB data

Data from 12 precipitation stations installed within and around the Mesochora catchment were considered for the period from 1971–1972 to 1985–1986 (Mimikou et al., 1991). Some of the station daily records included incomplete data, which were interpolated from corresponding data of neighbouring stations. The summation of daily values for every month yielded the monthly precipitation values, which in turn were averaged over the catchment area by the Thiessen method. The resulting areal monthly precipitation was used as input to the MWB model.

The temperature data were collected from the stations in the study region (the number of stations was not determined) (Mimikou et al., 1991). The monthly temperature values were obtained from the mean temperature of the stations corrected for the mean catchment elevation through a monthly lapse rate. Then, the catchment monthly temperature values were used in the MWB model for separating precipitation into rain or snow, and for use in the snowmelt algorithm. Furthermore, they were used to calculate the PET.

Monthly PET was also a direct input to the MWB model, and it was estimated according to the Blaney Criddle method (FAO, 1977). Data used in the PET algorithm were the relative humidity, relative sunshine duration, daytime windspeed and air temperature.

Three magnitude classes of monthly minimum relative humidity were obtained from data collected in situ. The monthly relative sunshine duration over the catchment was computed by averaging the records of two stations which were installed on both sides of the catchment's midpoint. The mean monthly values of daily wind were used to estimate PET in the form of three broad classes of magnitude. The data for the above classification were obtained from one station with incomplete and poor-quality records. These data were treated to make them acceptable for use in the Blaney–Criddle method. Monthly streamflow values were required for MWB model calibration, and were obtained from the Mesochora gauge station.

3.2. SAA–SMA data

Daily data from 11 precipitation stations, installed within and around the Mesochora catchment, were used in the SAA–SMA models. The precipitation stations are consistent

and representative of the catchment, but 3.5% of daily precipitation values were missing over the 15 year study period (1972–1986). To preserve the real nature of precipitation series and to avoid computational errors introduced by data filling methods, the missing data were not interpolated. Thus, the technique used to estimate the mean areal daily precipitation was a combination of the Thiessen method and availability of the station data, including elevation correction (Panagoulia, 1992b, 1994, 1995; Panagoulia and Dimou, 1995). The great importance given to the accurate integration of precipitation over area and elevation (as for the temperature integration described below) is necessary for the SMA model operation, which is based on an input-driven numerical difference scheme (Section 2.2).

Daily temperature data were obtained from three stations. One is installed inside the catchment, whereas the other two are installed outside. Of the daily maximum and minimum values over the 15 year study period (1972–1986), 15.5% are missing. The consistency of the data was checked by the double-mass curve on a monthly basis (Anderson, 1973), and the inconsistent data were corrected by applying an appropriate correction factor. For the same reasons, the missing daily maximum and minimum values were not interpolated and the mean areal maximum and minimum daily temperature was estimated through a technique combining the Thiessen method and the availability of the station daily data, including elevation correction (Panagoulia, 1992b, 1994).

To obtain the catchment monthly PET, the sunshine, temperature and humidity data were considered. The catchment sunshine was calculated as the monthly arithmetic average of the sunshine measurements of two stations installed outside the catchment near the eastern and western boundary. The catchment humidity was also calculated by arithmetic averaging of monthly data from two other stations, both installed outside the catchment near the western boundary.

The monthly temperature of the catchment was estimated using a combination of the Thiessen method and the availability of the monthly station data. The areal temperature was corrected for elevation variation by applying a monthly dependent lapse rate. The long-term monthly mean sunshine, temperature and humidity of the catchment were used as inputs to the Penman equation (Veihmeyer, 1964) to estimate the PET of the catchment. Other inputs to the Penman equation were the average wind speed (200 miles day^{-1}), the monthly percentage of reflecting surface and the solar radiation for the catchment's midpoint latitude. The monthly PET was disaggregated by the SMA model into daily increments.

The daily streamflow data of the Mesochora station were used for the period 1972–1986. Most of the streamflow records were complete, but some daily data were missing. To estimate the missing data a downward station was used as a backup station. The Mesochora missing data were estimated by multiplying the complete daily data of the downward station by the ratio of the monthly average streamflow. Details of the stations and their data quality, as well as the data filling methods used, have been presented by Panagoulia (1992b, 1994, 1995) and Panagoulia and Dimou (1995).

4. Model calibration

The procedures of model calibration, validation and verification are described below.

Table 1
MWB parameter description and parameter final values

Parameter	Description		Final value
SRC	Storm runoff coefficient (%)	October	0.20
		November	0.30
		December	0.30
		January	0.20
		February	0.20
		March	0.30
		April	0.30
		May	0.30
		June	0.20
		July	0.10
		August	0.05
		September	0.05
S_{max}	Maximum soil moisture		300 mm
T_0	Delineation temperature for maximum snow content		–3.5°C
T_1	Delineation temperature for precipitation falling entirely as rain		2°C
α	Minimum rain content coefficient		0.30
DF	Melt-rate factor		0.45 mm $°C^{-1}$ day^{-1}
K_1	Watershed lag coefficient		0.60
K_2	Groundwater reservoir coefficient		0.50

4.1. MWB calibration

The model was calibrated for 15 hydrological years, from 1971–1972 to 1985–1986 (the whole study period). The calibration was carried out by a series of trials of reasonable values for the entire Mesochora catchment. The model parameters which were subjected to calibration, as well as their final values, are given in Table 1.

The efficiency measure of calibration was based on the Nash parameter NTD (WMO, 1986), given by the formula

$$\mathrm{NTD} = 1 - \frac{\sum_{j=1}^{12} (Q_{sj} - Q_j)^2}{\sum_{j=1}^{12} (Q_j - \bar{Q})^2}$$

where Q_{sj} and Q_j are simulated and measured monthly streamflow, respectively, for each month of a hydrological year, and $\bar{Q}$ is the arithmetic mean of Q_j ($j = 1,\ldots,12$).

The average value of the Nash criterion for the calibration period was 0.864 for a maximum value of 1.00. The accuracy obtained was considered satisfactory by Mimikou and Kouvopoulos (1991) and Mimikou et al. (1991). In addition to the NTD criterion, a visual comparison between simulated and measured streamflow for only two hydrological years (1972–1973 to 1974–1975) has been performed. For this period, the monthly simulated runoff is in good agreement with the corresponding measured one. This 2 year display is insufficient to draw firm conclusions about the MWB calibration accuracy (MWB validation).

Table 2
SAA parameter description and calibrated parameter values

Parameter	Description	Calibrated value
SCF	A multiplying factor to correct for gauge catchment deficiency in the case of snowfall	1.10
MFMAX	Maximum melt factor during non-rain periods, which occurs on 21 June	0.90 mm $°C^{-1}$ per 6 h
MFMIN	Minimum melt factor during non-rain periods, which occurs on 21 December	0.40 mm $°C^{-1}$ per 6 h
UADJ	Average wind function during rain on snow periods	0.10 mm $mbar^{-1}$ per 6 h
SI	Mean areal water-equivalent above which there is always 100% areal snow cover	100 mm
NMF	Maximum negative melt factor	0.12 mm_e $°C^{-1}$ per 6 h
TIMP	Antecedent temperature index parameter	0.30
PXTEMP	Temperature which delineates rain from snow	1–0°C
MBASE	Base temperature for snow melt computation during non-rain periods	0°C
PLWHC	Per cent liquid-water-holding capacity of ripe snow	0.05
PAYGM	Average daily ground melt at the snow–soil interface	0.020 mm
EFC	Per cent area over which evapotranspiration occurs for 100% snow cover	0.61

Regarding the verification of the MWB model, the calibration period was divided into three subperiods with different precipitation trends. The model was implemented for each subperiod and the three different average values of NTD were calculated. The null hypothesis of the average NTD difference between two subperiods and any subperiod and calibration period was tested. All the hypotheses were accepted at the 95% confidence level. A detailed description of the model calibration, validation and verification has been given by Mimikou et al. (1991).

4.2. SAA–SMA model calibration

For the better performance of the SAA model, the Mesochora catchment was divided into three elevation zones. The daily rain plus melt (pseudo-precipitation) was averaged over the elevation zone areas. The SAA and SMA models were manually calibrated over the 15 year period (1972–1986) through a trial-and-error approach, which was carried out concurrently for both models. The initial estimates of model parameters were based on the hydrograph characteristics, climate and observed catchment features. The final scheme for making initial parameter estimates was that suggested by Anderson (1973) for the SAA model and that suggested by Peck (1976) for the SMA model. The description of the SAA and SMA model parameters and their calibrated values are shown in Table 2 and Table 3, respectively.

The statistics (standard error, average bias, mean, etc.) of the error analysis of daily flow and its components (surface, upper level, lower level), as well as the statistics of 3 day volume error analysis, including peaks, showed that the SAA and SMA models are capable of accurately reproducing the observed streamflow (the SAA model indirectly and the SMA model directly). However, some discrepancies were noted, which were related to antecedent dry conditions and extreme rainfalls. The typical monthly simulation errors,

Table 3
SMA parameter description and calibrated parameter values

Soil moisture phase	Parameter	Description	Calibrated value
Direct runoff	PCTIM	Minimum impervious catchment	0.01
	ADIMP	Additional impervious catchment	0.01
	SARVA	Catchment covered by streams, lakes and riparian vegetation	0.0
Upper zone	UZTWM	Upper zone tension water capacity	4.50 cm
	UZFWM	Upper zone free water capacity	4.61 cm
	UZK	Daily upper zone free water drainage rate	0.57
Percolation	ZPERC	Proportional increase in percolation from saturated to dry condition	6.00
	REXP	Exponent affecting the rate of change of percolation between wet and dry conditions	1.80
Lower zone	LZTWM	Lower zone tension water capacity	25.00 cm
	LZFSM	Lower zone supplementary free water capacity	9.00 cm
	LZFPM	Lower zone primary freewater capacity	30.00
	LZSK	Daily lower zone supplementary free water drainage rate	0.15
	LZPK	Daily lower zone primary free water drainage rate	0.015
	PFREE	Percolation water fraction passing directly to lower zone free water	0.20
	RSERV	Fraction of lower zone free water unavailable for transpiration	0.10
	SIDE	Ratio of non-channel baseflow to channel baseflow	0.00
Initial water	UZTWC	Upper zone tension water content	4.50 cm
	UZFWC	Upper zone free water content	0.11 cm
	LZTWC	Lower zone tension water content	21.41 cm
	LZFSC	Lower zone supplementary free water content	0.088 cm
	LZFPC	Lower zone primary free water content	2.26 cm
	ADIMC	Tension water content of the additional impervious catchment	25.91 cm

expressed as a percentage of observed flows, were of the order of 10–15%, and were higher in low runoff months (August and September) and lower in high runoff months.

The verification of the SMA model (and hence the SAA model) was tested through a modified differentiation split sample test for three distinct periods with different climate conditions into which the long-term annual mean catchment pseudo-precipitation was divided. The H_0 null hypothesis of the difference of annual runoff standard deviation and monthly correlation coefficient between two climate periods, and between any climate period and the calibration period, was tested. The statistical parameter were within 95% of the critical region. Details of the calibration, validation and statistical verification of the SAA–SMA models have been presented by Panagoulia (1992b).

5. Comparison of models—historical conditions

Although there are many criteria for describing how well a particular model performs

the task for which it is employed (i.e. various statistical and graphical presentations), we are limited to those used by Mimikou and Kouvopoulos (1991) to compare the ability of the MWB model and the SAA–SMA model to simulate the catchment dynamics. Thus, for the calibration period (that is, the entire study period for both approaches), the NTD parameter criterion was calculated for the series simulated with the SAA–SMA models. The NTD efficiency measure mean value was 0.872, which shows that the SAA–SMA models were better calibrated. For the verification periods—the three distinct periods with different climate conditions—no comparison can be made, as Mimikou and Kouvopoulos (1991) did not give the NTD values for these periods, or any other information related to the NTD calculation (e.g. length of the periods, observed monthly flows, etc.). The test of null hypothesis H_0 of the NTD difference between two climate periods, and between any climate period and the calibration period, cannot be used as a comparison measure because the test results were within 95% of the critical region for both modelling approaches. No other graphical presentation of results (e.g. simulated vs. observed time series plot) was given by Mimikou et al. (1991).

The MWB output time series include the total runoff (without separation into surface, subsurface, etc.) and the soil moisture. For comparison purposes, the soil moisture content predictions from the SMA model's five conceptual zones were summed to form the cumulative soil moisture. The sum is expected to correspond to the moisture storage in the soil column (Gan and Burges, 1990; Lettenmaier and Gan, 1990), although it is not possible to relate the content of the individual soil moisture zones directly to physical parameters. Another SAA–SMA output which can be compared with the MWB output is the total runoff. The results are given at seasonal and monthly time scale for both the total runoff (Table 4) and the cumulative soil moisture (Table 5).

The runoff values presented in Table 4 for the MWB and SAA–SMA models are similar. From January to May the SAA–SMA values are slightly higher than those of the MWB, with the exception of the value in February, which is 18% higher. This could be due to the more dynamic representation of the snowmelting process in the SAA model. In June, the SAA–SMA runoff was less than the MWB predicted runoff. This is due to the higher values of winter runoff predicted by the SAA–SMA models. In the dry months (August and September), the MWB values are progressively lower than those of the SAA–SMA models, as the main component of the summer streamflow is the baseflow, of which the recharging rate for the MWB model is less ($K_2 = 0.5$) than that of the watershed drainage ($K_1 = 0.6$). The effect of the greater watershed drainage ($K_1 = 0.6$) is apparent in the rainy months (October, November and December), during which the MWB runoff values are also progressively higher than those of the SAA–SMA models. Furthermore, the values in Table 4 indicate a greater interannual runoff variability in the SAA–SMA predictions compared with the MWB ones.

Comparing the SAA–SMA and MWB runoff results, the most extreme runoff values are predicted by the SAA–SMA models, i.e. the summer and winter runoff values were respectively lower and higher than the corresponding MWB ones. The summer runoff values have been calculated as the sum of the June, July and August runoff values. Similarly, the winter runoff values have been calculated as the sum of the December, January and February runoff values.

The values in Table 5 indicate large differences in soil moisture between the MWB and

Table 4
MWB and SAA–SMA model predicted monthly and seasonal mean total runoff (in mm)

Season model	January	February	March	April	May	June	July	August	September	October	November	December	Summer	Winter
MWB	135	139	151	179	131	52	24	12	9	50	110	173	88	447
SAA–SMA	137	164	165	183	135	41	24	16	16	49	98	164	81	465

Table 5
MWB and SAA–SMA model predicted monthly and seasonal mean cumulative soil moisture (in mm)

Season model	January	February	March	April	May	June	July	August	September	October	November	December	Summer	Winter
MWB	300	300	300	300	288	190	70	14	28	132	177	295	91	298
SAA–SMA	382	402	419	427	421	370	252	160	115	121	212	328	261	371

SAA–SMA models. These may be due to the different ways in which the soil moisture is calculated. In the MWB model, the soil moisture is not discretized in soil layers, in contrast to the SAA–SMA soil moisture, which is accumulated from five soil layers (upper and lower).

The SAA–SMA soil moisture values are much higher than the MWB ones. They increase from September to April and decrease from April to September, showing a great interannual variability. The MWB soil moisture values increase from August to January, remain constant during January–April, and decrease from April to August.

Comparing the SAA–SMA and MWB soil moisture results, the SAA–SMA model predicted a value of summer soil moisture about three times higher than the MWB one, and a value of winter soil moisture about 25% higher than the MWB one. The summer soil moisture values have been calculated by averaging the soil moisture values of June, July and August, and the winter ones by averaging the soil moisture values of December, January and February.

6. Summary and conclusions

A thorough examination and comparison between the monthly water balance and the US NWS snow accumulation–ablation and soil moisture accounting models was carried out. These models have already been used by various workers for the same catchment (the Mesochora catchment in Central Greece), for hydrological regime predictions under historical and climate change conditions. There were substantial differences in model time resolution, structure and calibration procedure, as well as in the input data used and their reliability. The SAA and SMA models operate on finer time increments (the first at 6 h step and the second at daily step) compared with the monthly step of the MWB model. The finer time scale is more appropriate for simulating the medium-size and mountainous nature of the catchment.

The MWB model includes only a snow accumulation index and a roughly represented snowmelt algorithm (degree-day method), whereas the SAA model is an integrated model including important processes, such as detailed snow accumulation procedure, energy exchange at the snow–air interface, freezing of melt water, liquid water storage, ground melt, etc., which make the snow melting representation more realistic.

The parameterization of the SMA model is different from that of the MWB-runoff model. The discretization in five soil layers, the thorough representation of streamflow components and the fully mathematical description of the interlinked processes in the SMA model provide more detailed and realistic hydrological predictions than those of the MWB model.

Neither model included an automatic calibration procedure. The parameter estimation process was different in the SAA–SMA and MWB models (e.g. the catchment division into elevation zones included in the SAA model was not included in the MWB model). Possible errors in the parameter estimation could cause significant difference in the model behaviour because neither model has undergone objective calibration procedures. Therefore, the reliability of the SAA–SMA data has been extensively checked. Inconsistent and suspicious point data were excluded. To avoid the computational errors introduced by

interpolation methods, the incomplete records were not filled. A technique combining the Thiessen method and station availability was used to estimate the areal precipitation–temperature data, which in turn were corrected for elevation variation. This technique was not used for the MWB input data, whereas it is of great importance for the SMA model, which is operated on a input-driven numerical difference scheme. Furthermore, the NTD efficiency measure, which was the only available evaluation criterion for the MWB model, showed the superiority of the SAA–SMA models compared with the MWB model. It is believed that the SAA–SMA models can better represent the observed hydrological regime than the MWB model, as the former cannot adapt to poor data, whereas the latter can more closely fit data which may be in error (Linsley et al., 1988).

The numerical results from the model implementation on the same catchment under historical inputs indicated generally comparable monthly runoff values but greater inter-annual variability for the SAA–SMA models. In contrast, the soil moisture results were very different between the SAA–SMA and MWB models; this is mainly due to the very different parameterization of moisture storages (five soil layers for the SMA model and one for the MWB model).

References

Anderson, E.A., 1973. National Weather Service river forecast system. Snow accumulation and ablation model. NOAA Tech. Memo. NWS HYDRO 17. National Oceanic and Atmospheric Administration, Silver Spring, MD, 198 pp.

Bae, D.H. and Georgakakos, K.P., 1994. Climatic variability of soil water in the American Midwest: Part 1. Hydrological modeling. J. Hydrol., 162: 355–377.

BAHC Core Project Office, 1993. Biospheric aspects of the hydrological cycle. Rep. 27, Institut für Meteorologie, Freie Universität Berlin, 103 pp.

Becker, A., 1992. Criteria for a hydrologically sound structuring of large scale land surface process models. In: J.P. O'Kane (Editor) Advances in Theoretical Hydrology: Tribute to James Dooge. European Geophysical Society Series on Hydrological Sciences, pp. 97–111.

Becker, A. and Nemec, J., 1987. Macroscale hydrologic models in support to climate research. IAHS Publ., 168: 431–445.

Burnash, R.J.C., Ferral, R.L. and Macquire, R.A., 1973. A generalized streamflow simulation system in conceptual modelling for digital computers. US National Weather Service, Sacramento, CA.

Clarke, R.T., 1973. A review of some mathematical models used with observations on their calibration and use. J. Hydrol., 19: 1–20.

Dooge, J.C.I., 1982. The parameterization of hydrologic processes. In: P.S. Eagleson (Editor), Land Surface Processes in Atmospheric General Circulation Models. Cambridge University Press, New York, pp. 243–288.

Dooge, J.C.I., 1986. Scale problems in hydrology. University of Arizona, Tucson, 63 pp.

Dooge, J.C.I., 1992. Hydrological models and climate change. J. Geophys. Res., 97(D3): 2677–2686.

FAO, 1977. Crop water requirements. Irrig. Drain. Pap. 24. FAO, Rome.

Fleming, G., 1975. Computer Simulation Techniques in Hydrology. Elsevier, New York.

Franchini, M. and Pacciani, M., 1991. Comparative analysis of several conceptual rainfall–runoff models. J. Hydrol., 122: 161–219.

Gan, T.Y. and Burges, S.J., 1990. An assessment of a conceptual rainfall–runoff model's ability to represent the dynamics of small hypothetical catchments. 2. Hydrologic responses for normal and extreme rainfall. Water Resour. Res., 26(7): 1605–1619.

Georgakakos, K.P. and Bae, D.H., 1994. Climatic variability of soil water in the American Midwest: Part 2. Spatio-temporal analysis. J. Hydrol., 162: 379–390.

Gleick, P.H., 1986. Regional water availability and global climatic changes: the hydrologic consequences of increases in atmospheric CO_2 and other trace gases. Ph.D. Thesis, University of California, Berkeley.

Gleick, P.H., 1987. The development and testing of a water balance model for climate impact assessment: modeling the Sacramento Basin. Water Resour. Res., 23(6): 1049–1061.

Global Atmospheric Research Programme, 1972. Parameterization of sub-grid scale processes. Report of Study Group Conference, Leningrad, October 1972, Publ. 8.

Gupta, V.K. and Sorooshian, S., 1983. Uniqueness and observability of conceptual rainfall–runoff models parameters: the percolation process examined. Water Resour. Res., 19(1): 269–276.

Hayes, R.J., Popko, K.A. and Johnson, W.K. (Editors), 1980. Guide Manual for Preparation of Water Balances. US Army Corps of Engineers, Hydrologic Engineering Center, Davis, CA.

Klemes, V., 1990. The modelling of mountain hydrology: the ultimate challenge. IAHS Publ., 190: 29–43.

Lettenmaier, D.P. and Gan, T.Y., 1990. Hydrologic sensitivities of the Sacramento–San Joaquin River Basin, California, to global warming. Water Resour. Res., 26(1): 69–86.

Lettenmaier, D.P., Gan, T.Y. and Dawdy, D.R., 1988. Interpretation of hydrologic effects of climate change in the Sacramento–San Joaquin River Basin, California. Tech. Rep. 110, Dept. of Civil Eng., University of Washington, Seattle.

Linsley, R.K., Kohler, M.A. and Paulhus, J.L.H., 1988. Hydrology for Engineers. McGraw–Hill, New York, pp. 338–339.

Manley, R.E., 1978. Simulation of flows in ungaged basins. Hydrol. Sci. Bull., 23(1).

Mather, J.R., 1978. The climatic water budget in environmental analysis, Health Co., Lexington Books, Lexington, MS.

Mimikou, M.A. and Kouvopoulos, Y.S., 1991. Regional climate change impacts: I. Impacts on water resources. Hydrol. Sci. J., 36(3): 247–258.

Mimikou, M., Kouvopoulos, Y., Cavadias, G. and Vayianos, N., 1991. Regional hydrological effects of climate changes. J. Hydrol., 123: 119–146.

Nemec, J. and Kite, G.W., 1981. Mathematical model of the Upper Nile basin. In: Logistics and Benefits of using Mathematical Models of Hydrologic and Water Resource Systems. IIASA–Pergamon, Oxford, pp. 167–178.

Panagoulia, D., 1991. Hydrological response of a medium-sized mountainous catchment to climate changes. Hydrol. Sci. J., 36(6): 525–547.

Panagoulia, D., 1992a. Impacts of GISS-modelled climate changes on catchment hydrology. Hydrol. Sci. J., 37(2): 141–163.

Panagoulia, D., 1992b. Hydrological modelling of a medium-sized mountainous catchment from incomplete meteorological data. J. Hydrol., 137(1–4): 279–310.

Panagoulia, D., 1993. Catchment hydrological responses to climate changes calculated from incomplete climatological data. IAHS Publ., 123: 461–468.

Panagoulia, D., 1994. Catchment climatological data and climate change in continental Greece. In: 5th Int. Conf. ENVIROSOFT 94 Development and Application of Computer Techniques to Environmental Studies, San Francisco, CA, 16–18 November 1994.

Panagoulia, D., 1995. Assessment of daily catchment precipitation in mountainous regions for climate change interpretation. Hydrol. Sci. J., 40(3): 331–350.

Panagoulia, D. and Dimou, G., 1994a. Temporal scale effects on modelled catchment hydrological processes in respect of global climate change. In: A.C. Demetracopoulos, C.D. Hadjitheodorou and G.P. Korfiatis (Editors), Restoration and Protection of the Environment 2. Proc. Int. Conf., Patras, Greece, 24–26 August 1994. University of Patras Press, pp. 65–71.

Panagoulia, D. and Dimou, G., 1994b. Catchment tension moisture responses to climate changes assessed from incomplete climatological data. In: W.R. Blain and K.L. Katsifarakis (Editors), Hydraulic Engineering Software V: Water Resources and Distribution. Vol. 1, Proc. 5th Int. Conf. Hydraulic Engineering Software HYDROSOFT 94, Porto Carras, Greece, 21–23 September 1994. Computational Mechanics Publications, Southampton, UK, pp. 115–122.

Panagoulia, D. and Dimou, G., 1995. Assessment of daily catchment precipitation in mountainous regions for climate change interpretation. Oral presentation in 5th Int. Conf. on Precipitation (organized by University of Minnesota and NTUA), Elounda, Crete, 14–16 June 1995.

Panagoulia, D. and Dimou, G., 1997. Linking space–time scale in hydrological modelling with respect to global climate change: Part 2. Hydrological response for alternative climates. J. Hydrol., 194: 38–63.

Peck, E.L., 1976. Catchment modelling and initial parameter estimation for the National Weather Service Forecast System. NOAA Tech. Memo. NWS HYDRO 31. National Oceanic and Atmospheric Administration, Silver Spring, MD.

Silar, J., 1990. Surface water and groundwater interactions in mountainous areas. IAHS Publ., 190: 21–28.

Smagorinsky, J., 1974. Global atmospheric modelling and the numerical simulation of climate. In: W.M. Hess (Editor), Weather and Climate Modification. Wiley, New York, pp. 633–686.

Sunada, K., 1993. A study of scale effects on the estimation of maximum direct runoff rates using a catchment model. IAHS Publ., 212: 289–297.

Thornthwaite, G.W. and Mather, J.R., 1955. The water balance. Drexel Inst. Technol., Publications in Climatology, Laboratory of Climatology, VII, No. 1, 104 pp.

Thornthwaite, G.W. and Mather, J.R., 1957. Instructions and tables for computing the potential evapotranspiration and the water balance. Drexel Inst. Technol. Publications in Climatology, Laboratory of Climatology, X, No. 3, 311 pp.

Veihmeyer, F.J., 1964. Evapotranspiration. In: V.T. Chow (Editor), Handbook of Applied Hydrology. McGraw–Hill, New York.

WMO, 1975. Intercomparison of conceptual models in operational hydrological forecasting. Oper. Hydrol. Rep. 7, WMO 429, Geneva.

WMO, 1986. Intercomparison of models of snowmelt runoff. Oper. Hydrol. Rep. 23, WMO 646, Geneva.